*Chemistry, Physics and Technology of Surface. 2024. V. 15. N 4. P. 583-593*

*UDC 661.666 : 66.087* doi: 10.15407/hftp15.04.583

**Yu.V. Hrebelna [1, 2], M.I. Terets [1], E.M. Demianenko [1], A.G. Grebenyuk [1], N.V. Siharova [1], S.V. Zhuravskyi [1], O.M. Ignatenko [1], O.A. Cherniuk [1], Yu.I. Sementsov [1, 2], M.T. Kartel [1, 2]**

# PREPARATION OF HIGH PURITY THERMOEXFOLIATED GRAPHITE BY ELECTROCHEMICAL METHOD

*[1] Chuiko Institute of Surface Chemistry of National Academy of Sciences of Ukraine*
*17 General Naumov Str., Kyiv, 03164, Ukraine, E-mail: teretsmariya@gmail.com*
*[2] Ningbo Sino-Ukrainian New Materials Industrial Technologies Institute*
*Kechuang building, N777 Zhongguan road, Ningbo, 315211, P.R. China*

*Carbon materials with a graphite-like structure have the highest thermal stability in a non-oxidizing environment, sufficient structural strength, are easily processed, etc., and therefore they are widely used in various fields of technology. There are two methods of obtaining such materials: pyrolysis or carbonization of hydrocarbons and processing of natural graphite, so-called "thermo-expanded graphite technology" (TRG), which consists of successive reactions of intercalation, hydrolysis and heat treatment of natural graphite, leads to modification of the surface of TRG particles and provides the ability to their pressing and rolling on rollers to form dense materials. Natural graphite with a carbon content of 99.0–99.5 % by mass is used for the production of TRG, from which sealing materials are obtained for the equipment of enterprises of general industrial purpose: the fuel and energy complex, the petrochemical industry, utilities, etc. In the equipment of nuclear power plants, materials from TRG, of so-called "atomic purity", are used, in which the carbon content must be at least 99.85 % by mass. Therefore, the purpose of the work is to obtain thermally expanded graphite of high purity by the method of electrochemical oxidation and further purification of flotation-enriched graphite. The production process took place in two stages: electrochemical intercalation of graphite with concentrated sulfuric acid followed by hydrolysis, and chemical further purification using ammonium bifluoride and Trilon B as cleaning reagents. Combining into one process of electrochemical oxidation of graphite and its further purification allows obtaining high purity TRG with a carbon content of 99.94–99.96 % by mass.*

*In order to find the regularities of the interaction of Trilon B with metal ions included in the composition of graphite impurities, quantum chemical modeling of these processes was carried out.*

*The energy effect of the interaction of the iron (III) cation is greater in absolute value (–969.1 kJ/mol) than for the case with the aluminum cation (–748.3 kJ/mol) both in the aqueous medium and in the adsorbed state on the surface of the graphene plane (–816.9 for $Fe^{3+}$ and –621.2 kJ/mol for $Al^{3+}$).*

*Regardless of the nature of the cation, its interaction with Trilon B is thermodynamically more likely in an aqueous solution than in an adsorbed state on the surface of a graphene-like plane.*

***Keywords**: thermally expanded graphite, flotation-enriched graphite, ammonium bifluoride, Trilon B, electrochemical oxidation, density functional theory, cluster approximation*

## INTRODUCTION

Due to its unique physical and chemical properties, graphite is used in many fields: electronics and electrical engineering, chemical industry, metallurgy, energy, transport, cosmetics, construction, aviation and space industry. Separately, we can highlight the production of composites with graphite used as a filler for various materials to improve their mechanical and heat-conducting properties. Thus, graphite is used due to its unique properties, such as high electrical conductivity, chemical inertness, heat resistance, and high lubricating capacity.

In particular, electrochemical intercalation, described in works [1–4], is one of the environmentally friendly, resource- and energy-saving methods of obtaining graphite intercalation compounds (GIC) in controlled regimes.

The influence of electricity consumption on the synthesis of GIC and expansion temperature on various parameters of thermoexpanded graphite synthesized by electrochemical method with different amount of passed electricity from 10.83 to 40.00 A h/kg [1] is shown. It is noted that increasing the temperature of graphite expansion leads to an increase in volume, specific surface area, and pore volume up to 800 °C. Above this temperature, these parameters remained practically unchanged.

SEM images of TEG particles obtained at the expansion temperature of 1000 °C, but with different amounts of passed electricity, according to work [1], are presented in Fig. 1.

The wide range of applications of thermoexpanded graphite (TEG) requires not only the selection of optimal production conditions, but also the determination of the expansion coefficient. A significant number of studies, such as [5–9], are devoted to evaluation of the relationship between the size of precursor particles, the degree of expansion and the structure of pores.

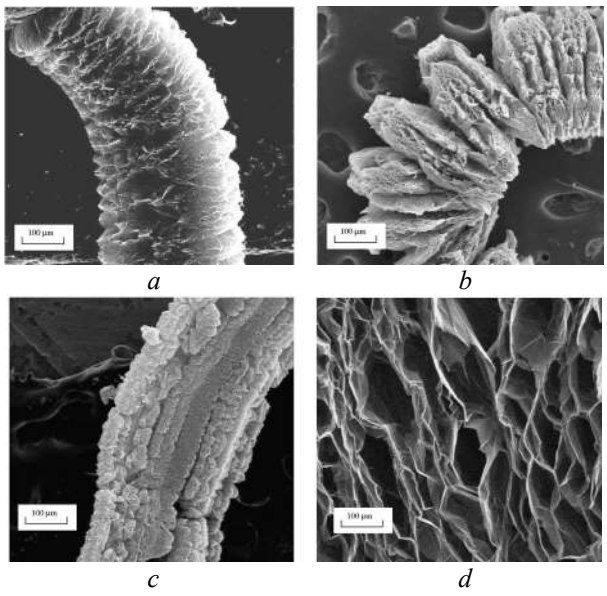


**Fig. 1.** SEM image of TEG particles: *a* – worm-shaped particles obtained from GIC with the amount of electricity passed through 33.33 A·h/kg; *b* – worm-shaped particles obtained from GIC with the amount of passed electricity of 10.83 A·h/kg; *c* – particles of residual compounds with 40 A·h/kg; *d* – cross-section of particles with internal pores

As can be seen from Figs. 2 and 3 [1], the amount of transmitted electricity significantly affects the specific surface area and pore volume, as well as the distance between adjacent exfoliated planes. An increase in the amount of passed electricity leads to an increase in the specific surface area, which leads to an increase in the total surface available for chemical reactions. An increase in the volume of pores is also observed, which indicates an increase in the porosity of the material. At the same time, the distance between the exfoliated GIC planes changes, which may be related to the intercalation of ions into the interplane space. These changes indicate structural modifications in the GIC under the action of electric current.

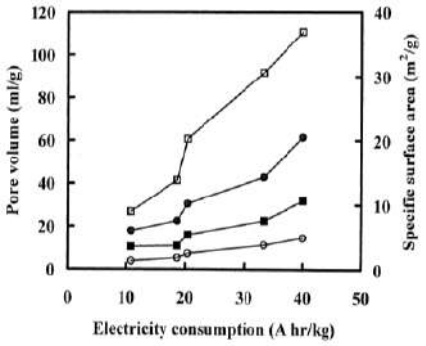


■ volume of pores with a radius of less than 4.5 μm;
□ volume of pores with a radius greater than 4.5 μm;
● specific surface area of pores with a radius of less than 4.5 μm;
○ specific surface area of cuts with a radius greater than 4.5 μm

**Fig. 2.** Dependence of the specific surface area and the volume of GIC on the amount of electricity passed

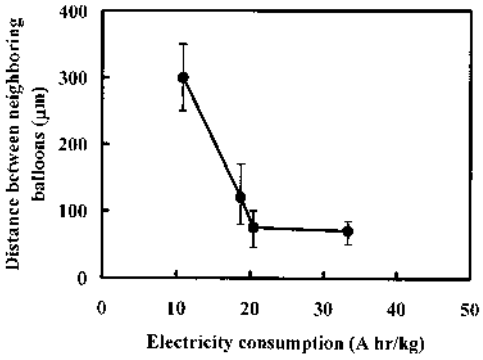


**Fig. 3.** Dependence of the change in the distance between adjacent delaminated planes on the transmitted electricity

In particular, the work [9] investigates the relationship between the coefficient of expansion and the porous structure of TEG by changing the conditions of the expansion temperature of natural graphite (keeping the crucible lid closed or open) with different sizes of precursor particles under the same conditions of their intercalation. It has been found that the TEG obtained from graphite float concentrate with a precursor particle size of 10 mesh (~ 1700 μm) has a low coefficient of expansion in the temperature range from 700 to 1100 °C, with the largest value at 1100 °C – 77 ml/g. The TEG obtained from graphite float concentrate with a precursor particle size of 50 mesh (~ 297 μm) has a significantly higher coefficient of expansion in the same temperature range as the previous sample, with the highest coefficient of expansion of 386 ml/g at 1100 °C.

## RESEARCH METHODS AND OBJECTS

***Experimental methods.*** Natural flotation-enriched graphite containing 94–97 % carbon is mixed with a sulfuric acid solution in the ratio of 50–100 $cm^3$ of electrolyte per 100 g of graphite. Sulfuric acid with a concentration of 94 % is used as an electrolyte. A mixture of graphite powder and electrolyte with a thickness of 4–10 mm is evenly distributed on the surface of the anode of the electrochemical reactor. A porous membrane made of chemically resistant polypropylene fabric is placed on the layer of the mixture of graphite powder and electrolyte, which is a good separator with low resistance to the movement of ions and has a sufficient thickness. A cathode under pressure is placed on a layer of polypropylene fabric, which provides electrical contact with the graphite powder. Then a direct current is passed through the graphite, the current density is 0.5–55 $mA/cm^2$, the amount of electricity consumed is 90–120 A·h/kg. After the end of the electrolysis process, the solid phase is separated from the solution. Then, a solution of ammonia to the alkaline reaction and a solution of the disodium salt of ethylenediaminetetraacetic acid are added to the solid phase at the rate of 5–40 g of salt per 100 g of graphite. The prepared mixture is heated to 50–100 °C for 1–2 hours. Then the solution is removed by filtration, washed with deionized water, and 2–4 % by weight is added. A solution of ammonium bifluoride in hydrochloric acid, which is taken at the rate of 10–20 g of ammonium bifluoride per 100 g of natural graphite, kept at a temperature of 55–75 °C for 5–10 hours, washed with deionized water until a negative reaction to chlorine ions, and the solid phase is separated from the solution, dried and heat-treated at a temperature of 800–1200 °C.

The work uses an experimental setup for the electrochemical synthesis of graphite, which is shown in Fig. 4.

In the second version, the sequence of addition of cleaning reagents was changed: ammonium bifluoride and Trilon B.

The content of metals in mineral impurities before and after graphite purification was determined using X-ray fluorescence analysis on a D8 ADVANCE diffractometer, manufactured by Bruker AXS, Germany.

***Methodology of quantum chemical calculations.*** A graphene-like plane (GP) with the general formula $C_{54}H_{18}$ (Fig. 5 *a*) was chosen as a model for graphene, which is the same size as the Trilon B molecule. In models of hydrated complexes, aluminum and iron (III) cations are surrounded by six water molecules (Fig. 5 *b*, *c*)

[11, 12]. In addition, since the electronic structure of the iron cation has a valence *d*-sublevel incompletely filled with electrons, it is necessary to find the spin state with the lowest energy for the hydrated complex with iron [13].

For this purpose, the hydrated complex of the iron(III) cation in spin states from 2 to 10 was calculated (Table 1). It should be noted that it was not possible to localize intermolecular complexes with a multiplicity of 8 and 10 without removing water molecules.

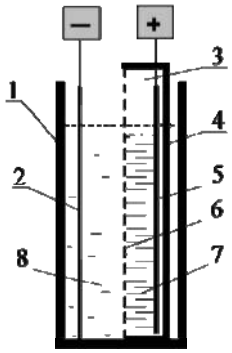


**Fig. 4.** Block diagram of an electrochemical reactor with a vertical arrangement of electrodes [10]: *1* – electrolytic bath, *2* – cathode, *3* – flat removable anode block, *4* – body of flat removable anode block, *5* – anode, *6* – membrane made of polypropylene fabric, *7* – natural flotation-enriched graphite, *8* – electrolyte

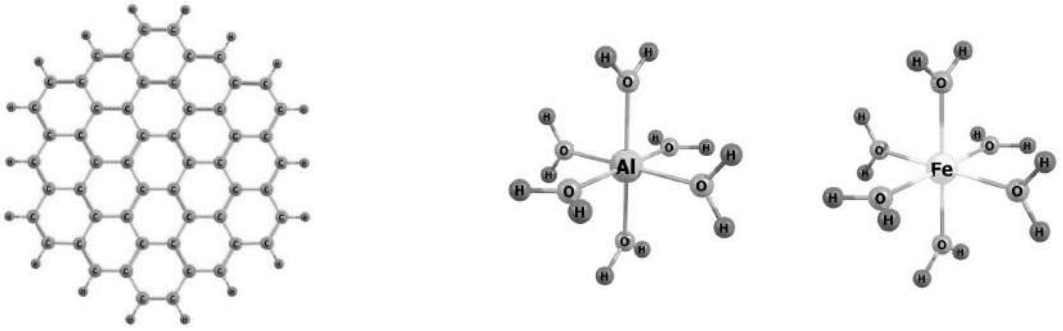


*a* *b* *c*

**Fig. 5.** Models for the graphene-like plane (*a*) of hydrated complexes of aluminum (*b*) and iron (*c*) cations

**Table 1.** Dependence of the total energy of the hydrated iron (III) cation complex on the spin state

| Multiplicity | Full Energy (Hartree) |
|---|---|
| 2 | -1721.1344868 |
| 4 | -1721.1425126 |
| 6 | -1721.1839955 |
| 8 | -1720.9869408 |
| 10 | -1720.7430449 |

As can be seen from the Table 1, the lowest value of the total energy is characteristic of the structure with multiplicity 6, therefore, in subsequent calculations, models with an iron(III) cation with this multiplicity were used.

Trilon B is a disodium salt of ethyldiamine-tetraacetic acid, which was sufficiently modeled in the literature [14–16].

Quantum chemical calculations were carried out using the GAMESS (US) program [17] by the density functional theory (DFT) method with the B3LYP functional [18, 19] and the 6-31G(d,p) basis set, taking into account the Grimme D3 dispersion correction [20, 21] within the PCM polarization continuum model [22, 23].

The complexation reaction of Al(III) and Fe(III) cations with Trilon B, which is considered here, can be represented by the general scheme (1):

$$[H_2EDTA(H_2O)_2]^{2-} + [Me(H_2O)_6]^{3+} \rightarrow$$

$$\rightarrow [MeEDTA]^{1-} + 2[(H_2O)_3\text{-}H_3O]^{1+}, \quad (1)$$

where Me are cations of Al(III) and Fe(III), $H_2EDTA(H_2O)_2]^{2-}$ is a partially hydrated Trilon B molecule, $[Me(H_2O)_6]^{3+}$ is a hydrated cation of Al(III) or Fe(III), $[MeEDTA]^{1-}$ is a metal complex with Trilon B, $[(H_2O)_3\text{-}H_3O]^{1+}$ is a hydrated hydroxonium cation.

The values of the energy effect of the interaction of Trilon B with $Me^{3+}$ cations in an aqueous solution were calculated according to formula (2):

$$\Delta E_{reac} = E_{tot}([MeEDTA]^{1-}) + 2E_{tot}([(H_2O)_3\text{-}H_3O]^{1+}) -$$

$$- E_{tot}([H_2EDTA(H_2O)_2]^{2-}) - E_{tot}([Me(H_2O)_6]^{3+}). \quad (2)$$

The energy effect of the interaction of Trilon B with hydrated $Me^{3+}$ cations adsorbed on the surface of GP was calculated using a formula similar to the one mentioned above, with the difference that, instead of $E_{tot}$ ($[MeEDTA]^{1-}$), the $E_{tot}$ of adsorbed complex ($GP\bullet\bullet\bullet[MeEDTA]^{1-}$) is concerned. The reaction products are eliminated in the experiment, so we also consider the desorption process from the surface of the graphene-like plane (3):

$$[H_2EDTA(H_2O)_2]^{2-} + GP\cdot[Me(H_2O)_6]^{3+} \rightarrow$$

$$[MeEDTA]^{1-} + 2[(H_2O)_6\text{-}H_3O]^{1+} + GP. \quad (3)$$

The energy effect of Trilon B interaction with hydrated $Me^{3+}$ cations adsorbed on the GP surface was calculated according to formula (4):

$$\Delta E_{reac} = E_{tot}([MeEDTA]^{1-}) + 2E_{tot}([(H_2O)_6\text{-}H_3O]^{1+}) +$$

$$+ E_{tot}([GP]) - E_{tot}([H_2EDTA(H_2O)_2]^{2-}) -$$

$$- E_{tot}(GP\cdots[Me(H_2O)_6]^{3+}). \quad (4)$$

## RESULTS AND DISCUSSION

***Electrochemical oxidation and further purification of flotation-enriched graphite.*** The paper developed the production of high purity TEG with the carbon content of more than 99.5 % by mass from flotation-enriched graphite (carbon content 94–97 % by weight). The production process took place simultaneously in two stages: electrochemical intercalation of graphite with concentrated sulfuric acid followed by hydrolysis, and chemical purification. A solution of ammonium bifluoride in sulfuric acid and Trilon B in an alkaline buffer were used as reagents for cleaning. Experimentally, it has been shown that this combination of electrochemical oxidation of graphite and its further purification into one process allows obtaining high-purity TEG with a carbon content of 99.94–99.96 % by mass and has great technological and economic advantages.

Note that the process of electrochemical intercalation is accompanied by reverse (or non-reverse) injection of mobile charged particles (cations and anions) from the electrolyte into the solid structure of the electrode. The course of this process significantly depends on such characteristics of the crystal lattice of the electrode material as the presence of voids for the transfer and placement of the intercalant, the mobility of intercalated ions in the electrode lattice, electronic conductivity and band structure, thermodynamic and kinetic stability of the electrode matrix during the intercalation process.

Schematically, the process of anodic oxidation is represented by the following scheme (5), where $i_i$ ($i_0$) is an intercalation (oxidation) current, NA is an acid.

It can be seen from the scheme that the process of intercalation and formation of graphite oxide is accompanied by the oxidation of the surface carbon atoms of the graphite electrode with gas evolution.

Thus, electrochemical intercalation reactions are limited by the degree of oxidation of the electrolyte (with the release of $O_2$) and the so-called phenomenon of graphite overoxidation, which depends on the nature of the electrolyte and the pH of the solution:

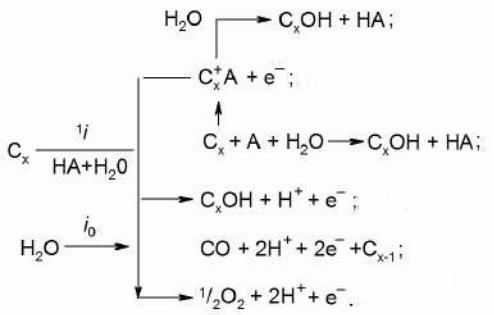

(5)

where $i_i$ ($i_0$) is an intercalation (oxidation) current, NA is an acid.

It can be seen from the scheme that the process of intercalation and formation of graphite oxide is accompanied by the oxidation of the surface carbon atoms of the graphite electrode with gas evolution.

It is most likely that during the peroxidation of graphite, covalent bonds of the C–OH type are formed, which is accompanied by a change in the aromatic structure of graphite with the formation of graphite oxide. Schematically, this reaction can be depicted as follows:

$$nC^+ + H_2O \rightarrow C_nOH + H^+ + e^- . \quad (6)$$

Schemes of anodic and cathodic processes during intercalation:

$$C_n + 3M^+X^- \rightarrow C_n{}^+X^- \cdot 2MX + M^+ + e^- , \quad (7)$$

$$C_n + 3M^+X^- \rightarrow C_n{}^-M^+ \cdot 2MX + X^- . \quad (8)$$

During anodic oxidation of graphite in concentrated acids (HA), graphite salts with the general formula are formed

$$C_n{}^+A_m{}^- \cdot HA \quad (9)$$

($n$ = 24, 48, 72 ….; $m$ = 2-2,5; $A^-$ is $HSO^-_4$).

The following anodic reaction of intercalation of sulfuric acid into graphite was established:

$$nC + HSO_4^- + mH_2SO_4 \leftrightarrows$$

$$\leftrightarrows C_n^+HSO_4^- \cdot mH_2SO_4 + e^- . \quad (10)$$

According to the literature data [24], the energy of the electrostatic interaction between the charged anion and the positively charged layers of graphite is approximately 209 kJ/mol.

The experimental parameters of electrochemical intercalation and purification of natural graphite by treatment with ammonium bifluoride + Trilon B are listed in Table 2.

The results of X-ray fluorescence analysis of samples of natural flotation-enriched and electrochemically oxidized and refined graphite are shown in Fig. 6. As can be seen from the figure, the use of ammonium bifluoride followed by the use of Trilon B contributes to more effective removal of impurities.

**Table 2.** Optimal parameters of electrochemical intercalation and purification of natural graphite by treatment with ammonium bifluoride + Trilon B

| Process parameters | Optimal values |
|---|---|
| Sulfuric acid concentration, % | 94 |
| Volume of sulfuric acid solution per 100 g of graphite, $cm^3$ | 50–100 |
| Current density, $mA/cm^2$ | 1–50 |
| Electricity consumption, A·h/kg | 80–120 |
| Consumption of EDTA per 100 g of graphite, g | 5–40 |
| Time of exposure of the mixture with EDTA, h | 1–2 |
| Holding temperature of the mixture with EDTA, h | 50–100 |
| Consumption of ammonium bifluoride per 100 g of graphite, g | 10–20 |
| Concentration of ammonium bifluoride, % by mass | 2–5 |
| Dwelling time of the mixture with ammonium bifluoride, h | 5–10 |
| Holding temperature of the mixture with ammonium bifluoride, ºC | 60–80 |
| Thermal shock temperature, ºC | 800–1200 |
| Carbon content, wt. % | 99.94–99.96 |

According to Fig. 6, the use of bifluoride ammonium and Trilone B, in order to further purify oxidized graphite, the value of Al cations decreased from 34.54 to 0.96 wt. %, and Fe from 24.86 to 0.65 wt. %.

As mentioned earlier, to obtain thermally expanded graphite, natural graphite is treated with concentrated sulfuric acid followed by washing with water [11]. As a result of this action on graphite during intercalation, the available metal oxides (which are polluting agents) are transformed into salts of sulfuric acid, in particular, $Al_2(SO_4)_3$ and $Fe_2(SO_4)_3$. In addition, the available iron(II) is further oxidized

to iron(III). Therefore, the charge of the considered cations is the same (+3), but of different nature ($Al^{3+}$ and $Fe^{3+}$). The cations of these salts are in a hydrated state and can be either in an adsorbed state on the surface of graphene planes, or in an aqueous medium between partially oxidized graphene planes. The mechanism of complexation and extraction of polluting metal cations ($Al^{3+}$, $Fe^{3+}$) by Trilon B is still unknown. Two cases of Trilon B interaction with these cations are possible: from an aqueous solution between the graphene planes of the intercalated graphite compound and in an adsorbed state on the surface of the graphene-like planes. Therefore, in order to clarify these features, the adsorption of Trilon B with the surface of graphene was investigated by quantum chemistry methods, and the geometric and energetic characteristics of the interaction between Trilon B with the corresponding hydrated cations of aluminum and iron (which are impurities in graphite) were found in an aqueous solution and in adsorbed state on a graphene-like plane.

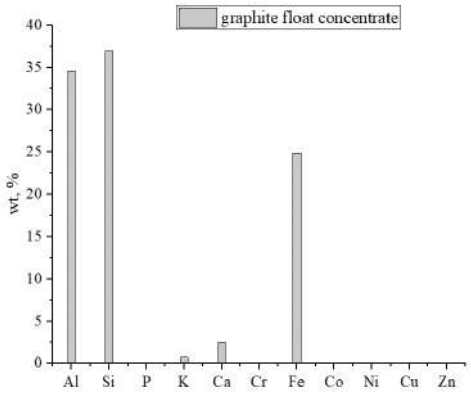


X-ray fluorescence analysis of graphite float concentrate

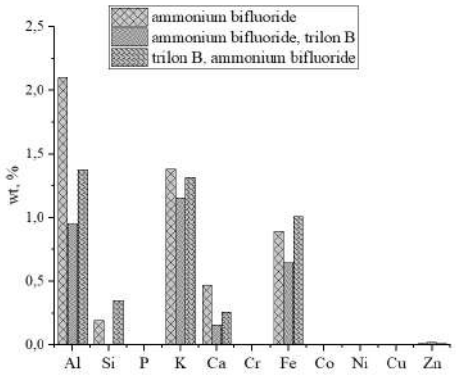


X-ray fluorescence analysis of oxidized graphite with additional purification: ammonium bifluoride; ammonium bifluoride, Trilon B; Trilon B, ammonium bifluoride

**Fig. 6.** Data of X-ray fluorescence analysis of samples of graphite float concentrate and oxidized graphite with additional purification

Thermally expanded graphite of the so-called "atomic purity" with a carbon content of 99.94–99.96 % by mass was obtained by electrochemical oxidation of graphite float concentrate (with a carbon content of 96 %) followed by its further purification using ammonium bifluoride and Trilon B.

***Quantum chemical calculations***. *Interaction of Trilon B with $Me^{3+}$ cations in an aqueous medium.* The first task was to investigate the reaction of complexation with the participation of partially hydrated Trilon B with hydrated $Me^{3+}$ cations, which occurs according to equation (1). In particular, in the case of aluminum, the equilibrium geometry of the starting compounds: Trilon B and aluminum cation was localized for this purpose (Fig. 7 *a*, *b*). The geometries of reaction products were also optimized, namely the Trilon B chelate complex with an aluminum cation (Fig. 7 *c*) and two hydrated hydroxonium cations (Fig. 7 *d*). Since Trilon B is a hexadentate ligand, it forms six coordination bonds with the aluminum cation [25], two of which involve amine nitrogen atoms and four with the participation of oxygen atoms of carboxyl groups of Trilon B.

The energy effect for this reaction, calculated according to formula (2), has a negative value (–748.3 kJ/mol, see Table 3), which indicates the thermodynamic probability of this reaction.

The interaction of Trilon B with the hydrated iron (III) cation with the formation, as in the previous case, of a complex with the $Fe^{3+}$ cation [25], which forms six coordination bonds, two of them involve nitrogen atoms of amino groups and four through participation of oxygen atoms of carboxyl groups of Trilon B. This reaction, like the previous one, occurs according to equation (1). There are localized equilibrium geometries of the participants of this reaction (Fig. 8), which are similar to those considered above. The $Fe^{3+}$ cation, both in the hydrated complex and with Trilon B, is in multiplicity 6.

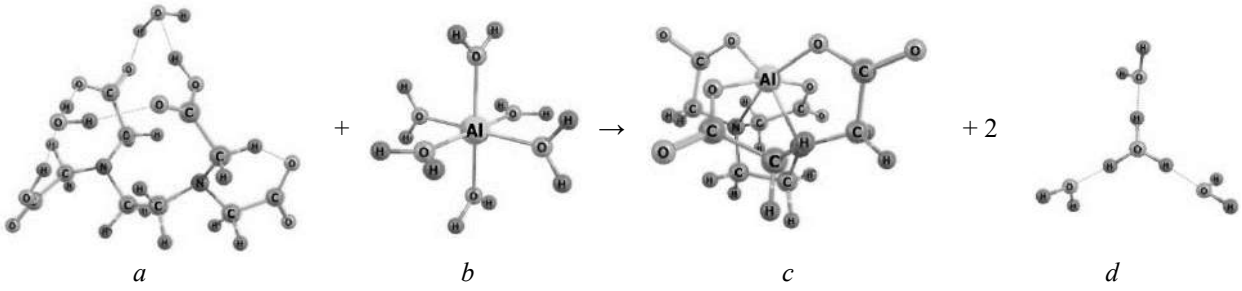


*a* *b* *c* *d*

**Fig. 7.** Equilibrium geometry of the reaction components of Trilon B (*a*) and hydrated aluminum cation (*b*) with the formation of a Trilon B chelate complex with aluminum cation (*c*) and hydrated hydroxonium cation (*d*)

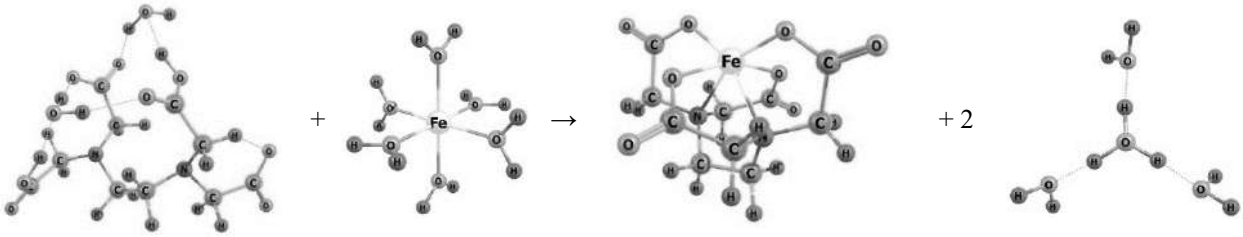


*a* *b* *c* *d*

**Fig. 8.** Equilibrium geometry of the reaction components of Trilon B (*a*) and hydrated iron(III) cation (*b*) with the formation of a chelate complex of Trilon B with iron(III) cation (*c*) and hydrated hydroxonium cation (*d*)

For this reaction, the energy effect calculated with formula (3) is also a negative value (–969.1 kJ/mol, see Table 3), and its value is 221 kJ/mol lower compared to the previous case.

*Interaction of Trilon B with hydrated aluminum(III) and iron(III) cations adsorbed on the surface of a graphene-like plane.* The next task was to find out the effect of GP on the reaction of complex formation during the interaction of adsorbed hydrated aluminum(III) and iron(III) cations. For this purpose, a partially hydrated Trilon B molecule (Fig. 9 *a*) interacts with the adsorbed complex of a hydrated aluminum cation (Fig. 9 *b*). In this adsorption complex, the water molecules of the hydrated aluminum cation complex are located at a distance of approximately 1.8 Å from the GP. The products of this reaction are precisely the chelate complex of Trilon B with an aluminum cation (Fig. 9 *c*) and two hydrated hydroxonium cations (Fig. 9 *d*), as in the previous cases, besides the product of this reaction is pure HP due to desorption (not shown in Fig. 9).

In the second case, similar to the previous one, the partially dissociated and hydrated Trilon B molecule (Fig. 10 *a*) interacts with the hydrated iron(III) cation, which is adsorbed on the GP (Fig. 10 *b*) (which is characterized by an intermolecular distance between adsorbent and adsorbate of approximately 2.1 Å). As a result, a chelate complex of Trilon B with an iron(III) cation (Fig. 10 *c*) and two hydrated hydroxonium cations (Fig. 10 *d*) is obtained, also as a product of the reaction there is pure GP due to desorption (in Fig. 10 is not shown).

The energy effects of these reactions, calculated according to formula (4), have values in the case of aluminum cation complexation –621.2 kJ/mol and –816.9 kJ/mol in the case of iron (III) cation complexation, respectively (see Table 3).

As can be seen from Table 3, the value of the energy effect of the interaction of magnesium and calcium cations with trilon B has a negative value both in the aqueous solution and in the adsorbed state on the oxidized GP. This testifies to the thermodynamic probability of this process in all considered cases. Regardless of the nature of the cation, its interaction with Trilon B is thermodynamically more likely in an aqueous solution than in the adsorbed state on the surface of the GP.

This Table also shows that both in aqueous solution and in the adsorbed state, the energy

effect of the interaction of the hydrated iron(III) cation with Trilon B is more significant compared to similar processes involving the hydrated aluminum cation.

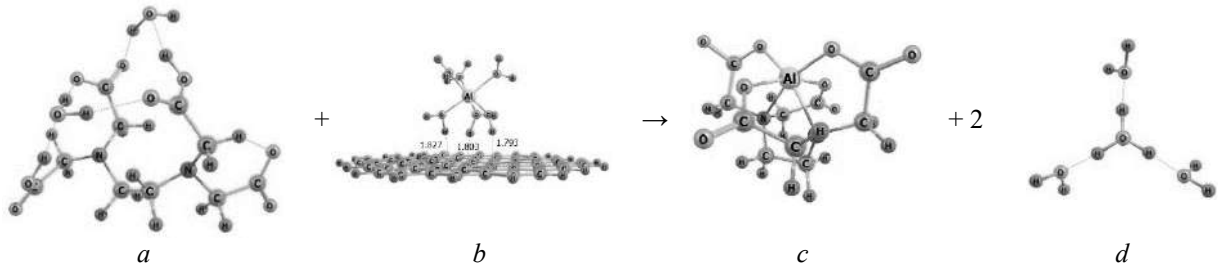


*a* *b* *c* *d*

**Fig. 9.** Equilibrium geometry of complexes of starting substances (*a*) and reaction product (*b*) for interaction of aluminum sulfate with Trilon B on the surface of a graphene-like plane

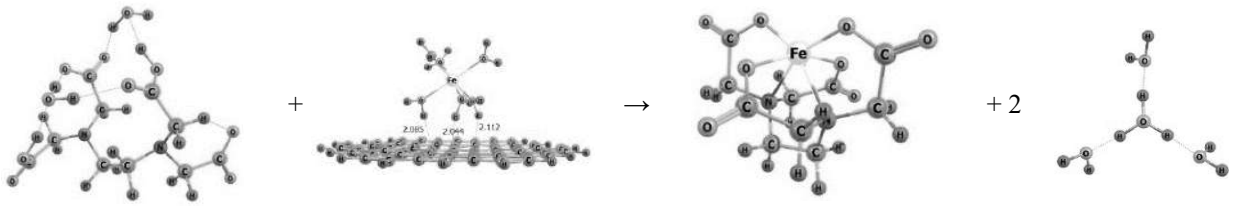


*a* *b* *c* *d*

**Fig. 10.** Equilibrium geometry of the components of the reaction of Trilon B (*a*) and the hydrated cation of iron(III) adsorbed on GP (*b*) with the formation of a chelate complex of Trilon B with the iron(III) cation (*c*), hydrated hydroxonium cation (*d*) and a graphene-like plane (not shown)

**Table 3.** Energetic effects of the interaction of aluminum and iron cations with Trilon B in an aqueous solution and in the adsorbed state on the surface of a graphene-like plane (in kJ/mol)

| | $Al^{3+}$ | $Fe^{3+}$ |
|---|---|---|
| Water solution | –748.3 | –969.1 |
| In the adsorbed state | –621.2 | –816.9 |

The calculated values of the energy effects of the interaction of these cations are confirmed by experimental results [26] about a higher complexation constant for $Fe^{3+}$ ($pK_{eq}$ ($Fe^{3+}$) = –25.1) compared to the similar value for $Al^{3+}$ ($pK_{eq}$ ($Al^{3+}$) = –16.3), which indicates the reliability data of quantum chemical calculations.

## CONCLUSIONS

It has been experimentally shown that the combination of the electrochemical oxidation of graphite and its further purification with ammonium bifluoride and Trilon B into one process allows obtaining high purity TEG with a carbon content of 99.94–99.96 % by weight. and has great technological advantages. Ammonium bifluoride ($NH_4HF_2$) chemically dissolves oxide and hydroxide impurities, after which Trilon B (EDTA) acts as a chelating agent that binds metal ions forming complex compounds with Trilon B, which are then removed from the electrolyte. As a result, the cleaning process does not damage the graphite structure, which is important for preserving its properties, and the method is environmentally safely, as it uses relatively safe chemical reagents.

The results of the analysis of quantum chemical calculations show that the values of the energy effect of the complexation of aluminum(III) and iron(III) cations with Trilon B have a negative value both in an aqueous solution and in the presence of a graphene-like plane. This indicates the thermodynamic probability of this process, which is consistent with the experimental results.

The energy effect of the interaction of the iron(III) cation is greater in absolute value (–969.1 kJ/mol) than for the case with the

aluminum(III) cation (–748.3 kJ/mol) both in the aqueous medium and in the adsorbed state on the surface of the graphene plane (–816.9 for $Fe^{3+}$ and –621.2 kJ/mol for $Al^{3+}$).

Regardless of the nature of the cation, its interaction with Trilon B is thermodynamically more likely in an aqueous solution than in an adsorbed state on the surface of a graphene-like plane.

## Отримання високочистого терморозширеного графіту електрохімічним методом

**Ю.В. Гребельна, М.І. Терець, Є.М. Дем'яненко, А.Г. Гребенюк, Н.В. Сігарьова, С.В. Журавський, О.М. Ігнатенко, О.А. Чернюк, Ю.І. Семенцов, М.Т. Картель**

*Інститут хімії поверхні ім. О.О. Чуйка Національної академії наук України*
*вул. Генерала Наумова, 17, Київ, 03164, Україна, teretsmariya@gmail.com*
*Китайсько-український інститут промислових технологій нових матеріалів*
*буд. Кечуанг, 777, Жонгуан роад, Ніньбо, 315211, Китай*

*Вуглецеві матеріали з графітоподібною структурою мають найбільшу термічну стійкість за неокисного середовища, достатню конструкційну міцність, легко обробляються.*

*Саме тому вони мають широке застосування в різних галузях техніки. Існують два методи одержання таких матеріалів: піроліз (карбонізація) вуглеводнів та переробка природного графіту - так звана «технологія терморозширеного графіту» (ТРГ), яка полягає в послідовних реакціях інтеркалювання, гідролізу та термообробки природного графіту. При цьому відбувається модифікація поверхні частинок ТРГ, що надає їм здатності до пресування та прокатування на вальцях з утворенням щільних матеріалів.*

*Для виробництва ТРГ, із якого одержують ущільнюючі матеріали для обладнання підприємств загальнопромислового призначення (паливно-енергетичного комплексу, нафтохімічної промисловості, комунальних господарств тощо), використовують природний графіт із вмістом вуглецю 99.0–99.5 мас. %. В той час як для обладнання атомних електростанцій потрібні матеріали з ТРГ так званої «атомної чистоти», в яких вміст вуглецю має бути не нижче 99.85 мас. %.*

*Тому метою роботи є розробка методики отримання терморозширеного графіту високої чистоти шляхом електрохімічного окиснення та доочистки флотаційно збагаченого графіту. Процес одержання складає два етапи: електрохімічне інтеркалювання графіту концентрованою сульфатною кислотою з подальшим гідролізом, і хімічна доочистка з використанням очищаючих реагентів - біфториду амонію та Трилону Б. Така доочистка електрохімічно окисненого графіту дозволяє одержати ТРГ високої чистоти з вмістом вуглецю 99.94–99.96 мас. %.*

*Для встановлення закономірностей взаємодії Трилону Б з іонами металів, що входять до складу домішок графіту, було проведено квантовохімічне моделювання цих процесів.*

*Енергетичний ефект взаємодії катіона заліза (III) за абсолютною величиною більший (–969.1 кДж/моль), ніж у випадку з катіоном алюмінію (–748.3 кДж/моль) як у водному середовищі, так і у адсорбованому стані на поверхні графенової площини (–816.9 для $Fe^{3+}$ і –621.2 кДж/моль для $Al^{3+}$).*

*Незалежно від природи катіона, його вилучення Трилоном-Б є більш енергетично вигідним з водного розчину, ніж з адсорбованого на поверхні графеноподібної площини стану.*

***Ключові слова**: терморозширений графіт, флотаційно збагачений графіт, біфторид амонію, трилон-б, електрохімічне окиснення, теорія функціонала густини, кластерне наближення*

REFERENCES

1. Kang F., Zheng Y.-P., Wang H.-N., Nishi Y., Inagaki M. Effect of preparation conditions on the characteristics of exfoliated graphite. *Carbon*. 2002. **40**(9): 1575.
2. Asghar H.M.A., Hussain S.N., Sattar H., Brown N.W., Roberts E.P.L. Potential Graphite Materials for the Synthesis of GICs. *Chem. Eng. Commun.* 2015. **202**(4): 508.

3. Abdillah O.B., Floweri O., Mayangsari T.R., Santosa S.P., Ogi T., Iskandar F. Effect of $H_2SO_4/H_2O_2$ pre-treatment on electrochemical properties of exfoliated graphite prepared by an electro-exfoliation method. *RSC Adv*. 2021. **11**(18): 10881.
4. Inagaki M., Iwashita N., Kouno E. Potential change with intercalation of sulfuric acid into graphite by chemical oxidation. *Carbon.* 1990. **28**(1): 49.
5. Goudarzi R., Hashemi Motlagh G. The effect of graphite intercalated compound particle size and exfoliation temperature on porosity and macromolecular diffusion in expanded graphite. *Heliyon.* 2019. **5**(10): e02595.
6. Liu T., Zhang R., Zhang X., Liu K., Liu Y., Yan P. One-step room-temperature preparation of expanded graphite. *Carbon.* 2017. **119**: 544.
7. Hristea G., Budrugeac P. Characterization of exfoliated graphite for heavy oil sorption. *J. Therm. Anal. Calorim.* 2008. **91**: 817.
8. Wang L., Fu X., Chang E., Wu H., Zhang K., Lei X., Yang Y. Preparation and Its Adsorptive Property of Modified Expanded Graphite Nanomaterials. *J. Chem.* 2014. **2014**(3): 1.
9. Çalın Ö., Kurt A., Çelik Y. Influence of expansionconditions and precursor flake size on porous structure of expanded graphite. *Fullerenes, Nanotubes and Carbon Nanostructures.* 2020. **28**(8): 611.
10. Sementsov Yu.I., Revo S.L., Ivanenko K.O., Hamamda S. *Expanded Graphite and Its Composites.* (Kyiv: PH "Akademperiodyka", 2019).
11. Evans R.J., Rustad J.R., Casey W.H. Calculating Geochemical Reaction Pathways - Exploration of the Inner-Sphere Water Exchange Mechanism in $Al(H_2O)_6^{3+}(aq) + nH_2O$ with ab Initio Calculations and Molecular Dynamics. *J. Phys. Chem.* A. 2008. **112**(17): 4125.
12. Esmaeilbeig M.A., Khorram M., Ayatollahi S., Zolghadr A.R. On the hydrolysis of ironions: DFT-based molecular dynamic perspective. *J. Mol. Liq*. 2022. **367**(Part A): 120323.
13. Zheng X., Wu X., Zhang L., Kang J., Zhou M., Zhong Y., Zhang J., Wang L. High spin $Fe^{3+}$-related bonding strength and electron transfer for sensitive and stable SERS detection. *Chem. Sci*. 2022. **13**(42): 12560.
14. Qinqin Yuan, Xiang-Tao Kong, Gao-Lei Hou, Ling Jiang, Xue-Bin Wang. Photoelectron spectroscopic and computational studies of $[EDTA{\cdot}M(III)]^-$ complexes (M = $H_3$, Al, Sc, V–Co). *Phys. Chem*. 2018. **20**(29): 19458.
15. Cendic M., Deeth R.J., Meetsma A., Garribba E., Sanna D., Matovic Z.D. Chelating properties of EDTA-type ligands containing six-membered backbone ring toward copper ion: Structure, EPR and TD-DFT evaluation. *Polyhedron*. 2017. **124**: 215.
16. Foreman M.M., Weber J.M. Ion Binding Site Structure and the role of water in alkaline earth EDTA complexes. *J. Phys. Chem. Lett*. 2022. **13**(36): 8558.
17. Barca G., Bertoni C., Carrington L. Recent developments in the general atomic and molecular electronic structure system. *J. Chem. Phys.* 2020. **152**: 154102.
18. Lee C., Yang W., Parr R.G. Development of the Colle-Salvetti correlation-energy formula into a functional of the electron density. *Phys. Rev. B*. 1988. **37**(2): 785.
19. Becke A.D. Density functional thermochemistry. III. The role of exact exchange. *J. Chem. Phys.* 1993. **98**(7): 5648.
20. Grimme S., Ehrlich S., Goerigk L. Effect of the damping function in dispersion corrected density functional theory. *J. Comput. Chem.* 2011. **32**(7): 1456.
21. Grimme S. Density functional theory with London dispersion corrections. *WIREs Comput. Mol. Sci.* 2011. **1**(2): 211.
22. Cossi M., Barone V., Cammi R., Tomasi J. Ab initio study of solvated molecules: a new implementation of the polarizable continuum model. *Chem. Phys. Lett*. 1996. **255**(4–6): 327.
23. Tomasi J., Mennucci B., Cammi R. Quantum Mechanical Continuum Solvation Models. *Chem. Rev.* 2005. **105**(8): 2999.
24. Chernysh I.G., Karpov I.I., Prikhod'ko G.P., Shai V.M. *Physicochemical properties of graphite and its compounds.* (Kyiv: Naukova Dumka, 1990). [in Russian].
25. Eckert S., Mascarenhas E.J., Mitzner R., Jay R.M., Pietzsch A., Fondell M., VazdaCruz V., Föhlisch A. From the Free Ligand to the Transition Metal Complex: $FeEDTA^-$ Formation Seen at Liga nd K-Edges. *Inorg. Chem*. 2022. **61**(27): 10321.
26. Roger Hart J. Ethylenediaminetetraacetic acid and related chelating agents. *Ullmann's Encyclopedia of Industrial Chemistry*. 2003. **13**: 573.


*Received 01.08.2024, accepted 25.11.2024*